Journal of Neurochemistry

JOURNAL OF NEUROCHEMISTRY | 2012 | 120 | 1084–1096 doi: 10.1111/j.1471-4159.2012.07657.x

ORIGINAL ARTICLE

Minimal essential length of *Clostridium botulinum* C3 peptides to enhance neuronal regenerative growth and connectivity in a non-enzymatic mode

Peter Loske,*[,1] Francesco Boato,†[,1,2] Sven Hendrix,† Johannes Piepgras,* Ingo Just,‡ Gudrun Ahnert-Hilger* and Markus Höltje*

*Center for Anatomy, Functional Cell Biology, Charité-Universitätsmedizin Berlin, Berlin, Germany
†Department of Morphology & BIOMED Institute, Hasselt University, Hasselt, Belgium
‡Institute of Toxicology, Hannover Medical School (MHH), Hannover, Germany

Abstract

C3 ADP-ribosyltransferase is a valuable tool to study Rho-dependent cellular processes. In the current study we investigated the impact of enzyme-deficient peptides derived from *Clostridium botulinum* C3 transferase in the context of neuronal process elongation and branching, synaptic connectivity, and putative beneficial effects on functional outcome following traumatic injury to the CNS. By screening a range of peptidic fragments, we identified three short peptides from C3bot that promoted axon and dendrite outgrowth in cultivated hippocampal neurons. Furthermore, one of these fragments, a 26-amino acid peptide covering the residues 156–181 enhanced synaptic connectivity in primary hippocampal culture. This peptide was also effective to foster axon outgrowth and re-innervation in organotypical brain slice culture. To evaluate the potential of the 26mer to foster repair mechanisms after CNS injury we applied this peptide to mice subjected to spinal cord injury by either compression impact or hemisection. A single local administration at the site of the lesion improved locomotor recovery. In addition, histological analysis revealed an increased serotonergic input to lumbar motoneurons in treated compared with control mice. Pull-down assays showed that lesion-induced up-regulation of RhoA activity within the spinal cord was largely blocked by C3bot peptides despite the lack of enzymatic activity.

Keywords: C3 transferase, regeneration, RhoA, spinal cord injury.

J. Neurochem. (2012) **120**, 1084–1096.

Clostridium botulinum produces the prototype of ADP-ribosylating C3 transferases (C3bot) that target RhoA, B and C proteins rendering them inactive (Aktories and Just 2005; Vogelsgesang *et al.* 2007). C3 transferases therefore represent a common tool to study Rho-dependent cellular functions. In neuroscience research, C3bot transferase has been demonstrated to promote axonal growth in primary neuronal culture (Jin and Strittmatter 1997), optic nerve lesion models (Lehmann *et al.* 1999; Bertrand *et al.* 2007) and experimental spinal cord injury (Dergham *et al.* 2002; Dubreuil *et al.* 2003). Over the years, evidence has accumulated that clostridial C3 transferase (C3bot) not only acts as an enzyme, but in addition is able to promote neurite outgrowth in a non-enzymatic mode of action (Ahnert-Hilger *et al.* 2004). Interestingly, application of enzyme-deficient C3bot, in which the catalytic amino acid glutamate at position 174 was mutated, resulted in growth promoting effects on hippocampal neurons. In subsequent studies, we successfully identified a 29-amino acid fragment covering the residues 154–182 ($C3bot^{154-182}$) still capable of inducing axonal as well as dendritic growth and branching in neuronal primary culture and organotypical brain slices (Höltje *et al.* 2009).

Received November 22, 2011; revised manuscript received January 8, 2012; accepted January 8, 2012.

Address correspondence and reprints request to Markus Höltje, Centrum für Anatomie, Institut für Integrative Neuroanatomie, Charité-Universitätsmedizin Berlin, Philippstr. 12, D-10115 Berlin, Germany.
E-mail: markus.hoeltje@charite.de

[1]These authors contributed equally to the manuscript.

[2]Present address: Université Pierre et Marie Curie, Institut de la Vision, Paris, France

Abbreviations used: 5-HT, 5-hydroxytryptamine; ARTT, ADP-ribosylation toxin-turn-turn; BMS, Basso Mouse Scale; CSPG, chondroitinsulfate proteoglycans; eGFP, enhanced green fluorescence; Map2, microtubule-associated protein 2; MEM, minimal essential medium; PBS, phosphate-buffered saline; SCI, spinal cord injury; VGAT, vesicular GABA transporter.

Furthermore, beneficial effects on axonal regeneration and functional recovery after spinal cord injury in mice were observed when this enzyme-deficient peptide was applied at the site of injury (Boato *et al.* 2010). To date, the exact molecular basis, by which enzyme-deficient C3bot peptides exhibit neurotrophic effects, remains to be elucidated. Also, important open questions regarding the use of C3bot peptides to foster neuronal regenerative growth still remain. This is, for instance, whether a motif such as the surface-exposed ADP-ribosylation toxin-turn-turn (ARTT) loop that confers substrate specificity and catalytic activity (Ménétrey *et al.* 2008) and is included in the 29-amino acid fragment is also essential for peptide action. Moreover, it is indispensable to gain more information about the minimal essential length of C3bot-derived peptides for exhibiting functional growth-promoting effects within the CNS. To minimise the risk for an unwanted immune response and to facilitate delivery in the *in vivo* situation the effective peptide should be designed as short as possible. We generated one peptide with a modified sequence, one C-terminal fragment and four further truncated C3bot peptides from the original sequence and tested them in a substantial range of both *in vitro* and *in vivo* models. The effects on neuronal morphology in culture, synaptic connectivity both in culture and the injured spinal cord, and the influence on axon growth in two different organotypical brain culture systems were investigated. Two different behavioural paradigms were applied to study the putative effects on motor restoration following spinal cord injury in mice. Last but not least, the impact of C3bot peptides on active RhoA levels within the injured spinal cord was analyzed.

Materials and methods

Animals

All *in vivo* experiments were done with Balb/C wild-type mice (females, 8- to 12-week-old) and were performed in accordance with German and Flemish guidelines on the use of laboratory animals.

Development of C3bot-derived peptides

$C3bot^{154-182\ E/Q}$ (C3bot 29mer E174Q), $C3bot^{154-182}$ (C3bot 29mer), $C3bot^{156-181}$ (C3bot 26mer), $C3bot^{160-179}$ (C3bot 20mer), $C3bot^{163-177}$ (C3bot 15mer) and $C3bot^{163-174}$ (C3bot 12mer) were synthesized at Pharis Biotec GmbH (Hannover, Germany). $C3bot^{181-211}$ (C3bot 31mer) was expressed as recombinant GST-fusion protein in Escherichia coli TG1 harboring the DNA fragment in the plasmid pGEX-2T. Peptides were reconstituted in phosphate-buffered saline (PBS) pH7.5, sterile filtered (0.22 μm) and used for the respective experiments.

Antibodies

Immunofluorescence

Monoclonal antibodies against neurofilament protein (200 kDa) and polyclonal antiserum against microtubule-associated proteins 2, were from Chemicon International (Hofheim, Germany). Rabbit or chicken anti-GFP antisera were used to further enhance green fluorescence (eGFP) (Invitrogen, Eugene, OR, USA). Synaptophysin-expressing terminals were visualized by a monoclonal anti-synaptophysin antibody (Synaptic Systems, Göttingen, Germany). Vesicular GABA transporter (VGAT) immunoreactivity was detected using guinea pig polyclonal serum (Calbiochem, Gibbstown, NJ, USA). Serotonin-positive boutons in spinal cord sections were detected by a polyclonal anti-5-hydroxytryptamine (5-HT) antiserum obtained from Immunostar (Hudson, WI, USA). Immunoreactivity was visualized using goat anti-mouse, goat anti-chicken Alexa Fluor 488, goat anti-rabbit Alexa Fluor 594, donkey anti-rabbit as well as donkey anti-guinea pig Cy3- and Cy5-coupled secondary antibodies (Molecular Probes, Eugene, OR, USA).

Immunoblotting

The Map2 and synaptophysin antisera were the same as used for immunofluorescence. A mouse monoclonal IgG from Cytoskeleton (Denver, CO, USA) was applied to detect RhoA. β-actin was detected by a polyclonal antiserum purchased from Sigma (St Louis, MO, USA).

Hippocampal cell culture

Hippocampal neurons were prepared from fetal NMRI mice at embryonic day 16 (E16). Dissected pieces of hippocampi were rinsed with PBS, then with dissociation medium [minimal essential medium (MEM) supplemented with 10% fetal calf serum, 100 IE insuline/l, 0.5 mM glutamine, 100 U/mL penicillin/streptomycin, 44 mM glucose and 10 mM HEPES buffer] and dissociated mechanically. Sedimented cells were resuspended in starter medium (serum-free neurobasal medium supplemented with B27, 0.5 mM glutamine, 100 U/mL penicillin/streptomycin and 25 μM glutamate) and plated at a density of $2x10^4$ cells/well (morphometrical analysis) or 8 x 10^4 cells/well (analysis of synaptic connectivity) on glass cover slips pre-coated with poly-L-lysine/collagen. An additional coating with 10 μg/mL chondroitin sulfate proteoglycans (Proteoglycan Mix; Millipore, Billerica, MA, USA) was performed in some experiments. All ingredients were obtained from Gibco/BRL Life Technologies, Eggenstein, Germany. One day after plating peptide fragments were added to the culture medium for the indicated time periods.

Morphometrical analysis

Total length and the overall number of branches from axons and dendrites were analyzed morphometrically using the Neurolucida software (MicroBrightField, Williston, ND, USA). The parameter 'axon length' represents the integral length of all visible parts of an axon, including all branches. Experiments were carried out on the basis of cultures prepared on the same day, from the same animal pool. Typically, three coverslips were prepared per condition and 8–10 neurons were evaluated on each coverslip. Provided no significant differences between coverslip means (tested by ANOVA) data were pooled and given as means ± SEM. Experiments were repeated at least three times following identical experimental protocols.

Analysis of synaptic connectivity

Detailed analysis was performed using the in-house written software NeMo 1.4, as described earlier (Henneberger *et al.* 2005). Briefly, hippocampal neurons cultured at high density were incubated with

or without C3bot peptides from DIV 4–7. Cultures were transfected with eGFP to visualize a low number of non-overlapping individual neurons using the Effectene Transfection Reagent (Qiagen, Hilden, Germany). After an expression period of 22 h cultures were fixed and stained for eGFP (to further enhance green fluorescence) and synaptophysin or the respective vesicular transmitter transporters. Labeled neurons were visualized by epifluorescence using a 63 times oil immersion objective. Stained terminals were quantified within a circular region of interest with a radius of 50 μm centered on the soma of an eGFP-labeled neuron. Only fluorescence spots with a diameter of 0.5–2 μm contacting a dendrite and supra-threshold intensity (average intensity plus three times its SD) were included in the analysis. In some experiments, synaptic contacts were counted in individual viewfields (area 350 × 262 μm) at 40 times magnification using untransfected cultures. Neurons were pooled from different coverslips for statistical analysis provided that significant differences between the coverslip means (tested by ANOVA) were absent. Pooled data were then compared using Student's *t*-test.

Organotypical brain slice culture and outgrowth assay

Entorhinal cortex slices were prepared at postnatal day 2 from mouse brains as described earlier (Hechler *et al.* 2006; Schmitt *et al.* 2007; Boato *et al.* 2010). Dissection of entorhinal cortex slices was performed in ice-cold MEM, with 2 mM L-glutamine and 8 mM Tris base added. Using a tissue chopper (Bachhofer, Reutlingen, Germany) transverse slices of 350 μm were cut. Slices were embedded in a collagen I matrix on glass slides. For cultivation, MEM supplemented with 25% Hank's Balanced Salt Solution, 25% heat-inactivated normal horse serum, 4 mM L-glutamine, 4 μg/mL insulin (Gibco, Karlsruhe, Germany), 2.4 mg/mL glucose (Braun, Melsungen, Germany), 0.1 mg/mL streptomycin, 100 U/mL penicillin and 800 ng/mL ascorbic acid (all from Sigma-Aldrich, Taufkirchen, Germany) was used. Cultures were kept at 37°C and 5% CO_2 for 48 h (with C3 peptides added) before microscopic analysis.

Axon counting

For measurement of axonal outgrowth from the explants, neurites of the explant were evaluated at a total magnification of 200, using a 20 times Olympus LCPLANFL objective (Olympus IX70, Hamburg, Germany). Axons that crossed a virtual line running at a distance of 100 μm parallel to the border of the concave explant side were counted.

Re-innervation assay

To analyze re-innervation of the denervated hippocampus *in vitro* an assay was used which combines an entorhinal cortex of a β-actin-eGFP+ mouse with a hippocampus of a wild-type littermate. The entorhinal-hippocampal eGFP slice cultures were prepared from mouse brains at day 2 post-partum as described elsewhere (Hechler *et al.* 2006). In brief, transverse hippocampal slices (350 μm) from wild-type animals were placed on membranes (Millicell-CM, Millipore, Eschborn, Germany) adjacent to eGFP+ entorhinal cortex slices, rearranging *in vitro* the correct anatomy of the hippocampal formation *in vivo*. The slices were kept at 5% CO_2 at 37 °C. The medium contained 50% MEM, 25% BME basal medium, 25% heat-inactivated normal horse serum, 2 mM glutamax (all Gibco) and 0.65% glucose (Braun), adjusted to pH 7.2. Slice co-cultures were treated for 48 h with C3bot peptides. After treatment, the entorhinal-hippocampal eGFP slices were fixed with 4% paraformaldehyde and 0.5% glutaraldehyde.

Measurement of axonal ingrowth (re-innervation)

To evaluate the axonal ingrowth from GFP-positive entorhinal cortices into the GFP-negative hippocampal target tissue, the GFP-labeled fibers, which had grown into the hippocampus, were photodocumented with a fluorescent microscope (Olympus BX50) and a Photometrics CoolSNAP^{TM}ES camera (VisitronSystems GmbH, Munich, Germany). Photomicrographs were then analyzed with MetaMorph Image Software (VisitronSystems GmbH) to determine the average intensity in a standardized area, including the interface entorhinal cortex/hippocampus and the perforant path. The values from the experimental cultures were compared with control cultures prepared in the same experiment. Subsequently, the data of multiple experiments were pooled for statistical analysis. After confirming that significant differences existed between groups by performing a Kruskal–Wallis Test, *p*-values (significance level of 0.05) were determined, using a Mann–Whitney *U* test (applies both to outgrowth and re-innervation assay).

Experimental spinal cord injury

Compression injury

Spinal cord compression injury was performed as described previously (Sieber-Blum *et al.* 2006; Boato *et al.* 2010). Briefly, 9- to 11-week-old anesthetized Balb/C mice (20–24 g) underwent a dorsal laminectomy at thoracic level T8, and a compression lesion was performed with a SPI Correx tension/compression gauge (Penn Tool, Maplewood, MN, USA) modified with the feeler bended to a 90 degree angle, and with a flat 1.25 mm tip designed to precisely fit in the cavity created by the laminectomy. Compression of the mouse spinal cord was then performed by two investigators (both blinded to experimental groups, one compressing the spinal cord and the other double checking pressure and time applied to each animal) at 20 cN for 1 s. Under these conditions, this injury type approximates the rapid force/acceleration injuries common to weight drop models. After positioning of the gelfoam patch on top of the perforated dura, the muscles were sutured and the back skin closed with wound clips.

Dorsal hemisection

For the spinal cord bilateral dorsal hemisection, iridectomy scissors were used to transect left and right dorsal funiculus, the dorsal horns (Simonen *et al.* 2003) and additionally the ventral funiculus (to cut also the small proportion of ventrally running corticospinal as well as raphespinal fibers close to the midline). Thus, the hemisection resulted in a complete transection of dorsal and medio-ventral descending fiber tracts (Boato *et al.* 2010). Following this procedure, mice were treated as described above. Both spinal cord injury (SCI) procedures were performed under a Leica MS5 stereo microscope.

Locomotion tests

Mice were continuously tested for functional recovery three weeks following SCI with the Basso Mouse Scale (BMS; Basso *et al.* 2006). The BMS is a 10-point locomotor rating scale (9 = normal locomotion; 0 = complete hind limb paralysis), in which mice are scored by two investigators blinded to experimental groups based on

hind limb movements made in an open field during a 4-min interval. After allowing mice to recover for 5 days, Rotarod performance (Sheng *et al.* 2004) was determined continuously up to the end of the observation periods. The mice were placed on an accelerated rolling rod (Ugo Basile, Comeris VA, Italy). The latency to jump off from the rod was automatically recorded by the action of the mouse dropping onto a trigger plate. For BMS analysis we used the mean of the left and right hindlimb scores for each animal. Rotarod and BMS data were analyzed using a two-way ANOVA as previously described (Basso *et al.* 2006) and represent mean values for all the animals of each experimental group ± SEM.

Rho GTPase pull-down assay

Pull-down assays to detect activated RhoA in spinal cord tissue were performed using a Rho activation assay kit according to manufacturer's instructions (Cytoskeleton, Denver, CO, USA). Briefly, dissected pieces of spinal cord of 1 cm length that included the lesioned area were obtained from PBS-perfused animals, homogenated and lysed in lysis buffer. The soluble fraction was obtained by centrifugation (10 500 *g* for 2 min). Aliquots were saved for analysis of total RhoA and loading control. Lysates were then added to rhotekin-RBD beads for 1 h (4°C). Pelleted beads were washed three times, and bound proteins were mobilized by incubation with Laemmli sample buffer at 95°C for 5 min. Samples were subjected to sodium dodecyl sulfate–polyacrylamide gel electrophoresis and western blot analysis.

Histological analysis of spinal cord tissue

Spinal cord cryosections (20 μm) from transcardially perfused animals were preincubated with 10% normal goat serum dissolved in PBS containing 0.5% Triton X-100 for 30 min at 20°C. Incubation with primary antibodies was carried out overnight at 4°C. Following repeated washing steps with PBS, secondary antibodies were applied for 2 h at 20°C. After removal of unbound antibodies, sections were mounted.

Quantification of GABAergic and serotonergic inputs to lumbar α-motoneurons

α-motorneurons of lumbar segments 1–2 (L1–L2) of the most ventral part of the ventral horn (representing Rexed's lamina 9) were analyzed. The number of VGAT-positive inputs (vesicular GABA transporter) and 5HT-positive boutons on motoneurons was calculated according to the criteria given elsewhere (Müllner *et al.* 2008). Briefly, 5HT-positive swellings and VGAT-positive spots directly contacting α-motoneuron somata were counted in relation to the cell body perimeter as measured by Leica Application Suite software (Leica Microsystems, Wetzlar, Germany). Measurements are expressed as number of boutons (spots) per 100 μm cell perimeter.

Results

To investigate putative growth-promoting effects of short peptides derived from *Clostridium botulinum* C3 transferase (C3bot) on hippocampal neurons, we generated different peptides from a sequence comprising the amino acids 154–182 known to exhibit neurotrophic activity (Höltje *et al.* 2009). In one of the peptides, the catalytic glutamate at position 174 was exchanged for glutamine (C3bot$^{154-182}$ E174Q referred to as C3bot 29mer E174Q). Four peptides represented further truncated versions of the original 29 amino acid sequence: C3bot$^{156-181}$ or C3bot 26mer, C3bot$^{160-179}$ or C3bot 20mer, C3bot$^{163-177}$ or C3bot 15mer and C3bot$^{163-174}$ or C3bot 12mer (Fig. 1a). Finally, a peptide that flanked the initial 29mer to the C-terminal end was used covering the amino acids 181–211 (C3bot 31mer). To test for beneficial effects on neuronal outgrowth murine hippocampal cultures kept under serum-free conditions were incubated with 50 nM of the respective peptides for four days. In contrast to full length C3bot, these peptides harbour no enzymatic activity as expected and already demonstrated for the initial 29mer (Höltje *et al.* 2009). Following incubation, fixed neurons were stained for axonal neurofilament protein and dendritic microtubule-associated protein 2 (Map2) as markers for axons and dendrites, respectively, and were morphometrically analysed. The rationale for the use of the modified 29mer peptide with glutamine instead of glutamate at position 174 (essential for catalytic function of full length protein), was to check whether this residue is also involved in peptide effects on neuronal morphology. Treatment of hippocampal neurons with C3bot 29mer E174Q indeed enhanced axon and dendrite length. Complexity of branching, on the other hand, was not significantly altered (Fig. 1b and e). The four further shortened peptides were designed to pinpoint the minimal length of C3bot-derived fragments to foster neuronal outgrowth with the shortest one reflecting the 12 amino acid of the ARTT loop responsible for substrate recognition of the full length C3bot transferase. In addition, the C-terminal 31mer was used to demonstrate whether an inclusion of substantial parts of the residues located between position 154 and 182 is essential for biological activity. Following incubation with the respective peptides two candidates exhibited promoting effects on neuronal process growth: C3bot 26mer (Fig. 1c and e) resulted in a significant promotion of axonal and dendritic length and, in addition, enhanced the complexity of branching in these two compartments. Application of the shorter C3bot 15mer also resulted in the promotion of axonal length and branching, effects on dendrite morphology, however, did not reach statistical significance (Fig. 1c and e). The other three peptides were without effects on the parameters studied. Therefore, the 29mer peptide seems to be effective even with an amino acid exchange at a critical position, and certain further truncated peptides still exhibit beneficial effects on the morphology of cultivated neurons. Next, we addressed the question whether the observed morphological effects elicited by the shorter C3bot 26mer and C3bot 15mer were accompanied by functional changes such as the number of synaptic inputs. To this end, we quantified the number of synaptophysin-positive terminals contacting the proximal dendrites of individual eGFP-transfected neurons (Fig. 2a). Using NeMo software (Henneberger *et al.* 2005)

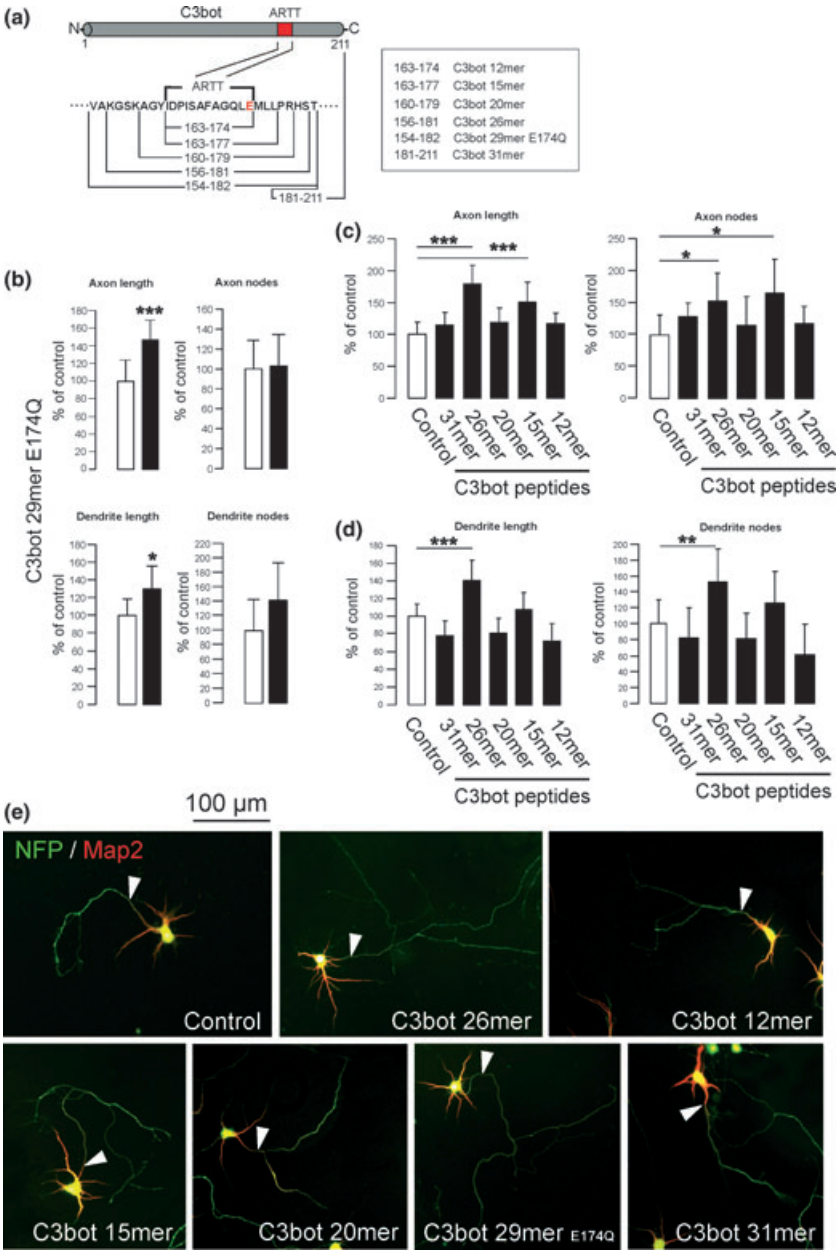

Fig. 1 Effects of C3bot peptides on the morphology of hippocampal neurons. (a) Schematic illustration of the various peptides generated from the sequence of clostridial C3 transferase (C3bot). C3bot$^{181–211}$ was expressed as recombinant protein, all other peptides were synthetically manufactured. ARTT: ADP-ribosylation toxin-turn-turn motif; E174: catalytic glutamate at position 174. (b) Hippocampal neurons were prepared at embryonic day 16 and cultivated for 4 days under serum-free conditions with 50 nM of C3bot 29mer E174Q. Neurons were fixed and double stained for neurofilament protein (NFP) as axonal and microtubule associated protein 2 (Map2) as dendritic marker. Axonal and dendritic process length and branch nodes were morphometrically quantified using Neurolucida software. Incubation with C3bot 29mer E174Q significantly increased axonal length and dendritic length but did not significantly affect branching. (c, d) Application of the 31mer and further shortened peptides for 4 days at 50nM. Incubation with C3bot 26mer significantly increased all parameters. C3bot 15mer had beneficial effects on axonal length and branching. C3bot 31mer, 20mer and 12mer were without significant effects. $N = 3$ or more experiments, data were taken from a representative experiment. Data shown are from 25 neurons per condition. Statistical significance was verified using Student's *t*-test. $^{*}p < 0.05$; $^{**}p < 0.005$; $^{***}p < 0.001$. (e) Photomicrographs illustrating the effects of the different peptides in double-stained hippocampal culture.

synaptophysin-expressing inputs that contacted proximal dendrites were counted based on size and intensity criteria. Incubation with C3bot 26mer enhanced the level of connectivity by about 50% (Fig. 2b and c). Accompanying Western blot analysis confirmed an increased expression of synaptophysin together with a higher level of dendritic Map2 expression in cultures treated with C3bot 26mer (Fig. 2d). Despite its beneficial effects at least on axonal morphology C3bot 15mer was without effect on the number of synaptic inputs (Fig. 2e). Also, incubation with C3bot 20mer or C3bot 12mer did not result in any detectable effects on general synaptic connectivity in culture as tested for non-transfected neurons (Figure S1, C3bot 26mer was used as positive control). To investigate the efficacy of C3bot peptides to act also on growth-inhibitory substrate we cultivated hippocampal cultures on extracellular matrix constituents such as chondroitinsulfate proteoglycans (CSPG), which are strongly secreted in response to lesions of the CNS. CSPGs are known to act as RhoA activators (Schweigreiter *et al.* 2004). The growth of hippocampal neurons on CSPG substrate exhibited a reduced morphological complexity (Fig. 2f) and, presumably as a consequence of that, also expressed less synaptic contacts than neurons grown on normal substrate (Fig. 2g). Incubation with C3bot 26mer, but not C3bot 15mer, however, prevented this CSPG-induced loss of synaptic contacts (Fig. 2g). So, albeit lacking

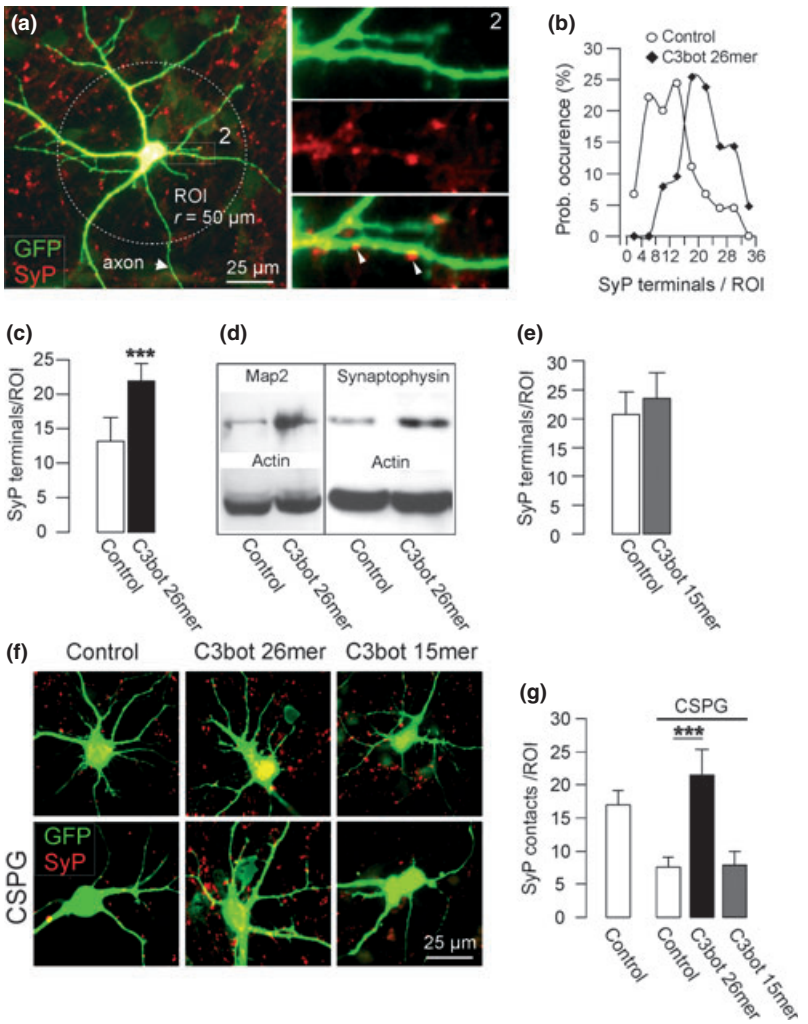

Fig. 2 C3bot 26mer but not C3bot 15mer increases the number of synaptic connections in hippocampal culture. (a) Sample pictures of an eGFP-transfected hippocampal neuron at DIV 6 immunostained against green fluorescent protein (GFP) and the synaptic marker protein synaptophysin (SyP). The number of synaptophysin-positive inputs was quantified on proximal dendrites within a circular region of interest at a radius of 50 µm centered on the soma of the cell. The boxed area in the merged picture is enlarged and depicts typical synaptophysin-positive terminals (arrowheads) contacting dendrites of the transfected neuron. (b) Histogram of data from neurons treated for 4 days with 50 nM C3bot 26mer indicating the relative occurrence of SyP terminals within individual regions of interest. Terminal counts were class-divided (nine classes, *x*-axis) and plotted against the percentage of neurons that exhibited the respective number of counts (probability of occurrence in %). C3bot 26mer shifts the number of inputs to higher values. $N = 3$ or more experiments, data were taken from a representative experiment. Data shown are from 45 (control) and 63 neurons (C3bot 26mer). (c) C3bot significantly increases the number of SyP terminals by around 50% compared with untreated neurons. Primary data were the same as in panel (b). (d) Western blot analysis of the effects of 50 nM C3bot 26mer on the expression of Map2 and synaptophysin. Both proteins were found to be up-regulated and support the observations shown in Fig. 1c and the current figure. (e) In contrast to C3bot 26mer, the shorter peptide C3bot 15mer (50 nM) did not affect the number of synaptophysin-expressing terminals. $N = 3$ or more experiments, data were taken from a representative experiment. Data shown are from 29 (control) and 30 neurons (C3bot 15mer). Experiments were repeated at least three times. (f, g) Parallel cultures were cultivated on growth-inhibitory chondroitinsulfate proteoglycans (CSPG) substrate and synaptic contacts were counted. Incubation with C3bot 26mer was able to prevent the observed strong down-regulation of synaptic inputs in cultures grown on CSPG substrate. C3bot 15mer was without effect. $N = 3$ or more experiments, data were taken from a representative experiment. Data shown are from 68 (control), 45 (control CSPG), 28 (C3bot 26mer CSPG) and 24 neurons (C3bot 15mer CSPG) respectively. (c, g) Statistical significance was verified using Student's *t*-test. ***$p < 0.001$.

enzymatic activity to inhibit Rho proteins, C3bot 26mer seems to mediate its effects on synaptic connectivity by interference with RhoA activation.

Organotypical brain slice culture is an established model to evaluate the influence of drugs on axonal outgrowth or re-innervation (Hechler *et al.* 2010; Schmitt *et al.* 2010). It

resembles more closely the *in vivo* situation than dissociation culture since all the cell populations of the brain are present in the brain explants, and additionally it allows for a more exact control of experimental conditions than in the animal model. Murine entorhinal cortex explant cultures (Fig. 3a and b) were then incubated with medium only, C3bot 26mer or C3bot 15mer for 48 h. Subsequently, the number of outgrowing axons comprising the perforant path in the intact brain was quantified. Incubation with C3bot 26mer enhanced the number of axons by 35% compared with control conditions (Fig. 3c and d). Treatment with C3bot 15mer on the other hand was without any effect. Another organotypical culture system was used to investigate the growth-promoting effects of C3bot peptides: we applied an eGFP/wild-type co-culture model that combines the entorhinal cortex of a β-actin-eGFP mouse with the hippocampus of a wild-type mouse. eGFP-expressing axons of the perforant path were clearly detectable and quantifiable in the non-fluorescent wild-type hippocampus. Slices were treated as described for the outgrowth model. An increased re-innervation of the hippocampus by perforant path fibers was detected after application of C3bot 26mer (measured as an increase in fluorescence intensity by 50%). Again, no effects were observed for C3bot 15mer (Fig. 3e and f).

In the light of these findings, we refrained from a further use of C3bot 15mer and, instead, applied the more promising 26mer in the subsequent *in vivo* experiments. Using either compression injury model of the spinal cord or a dorsal hemisection lesion paradigm at thoracic level T8 we tested for beneficial effects of C3bot 26mer on the

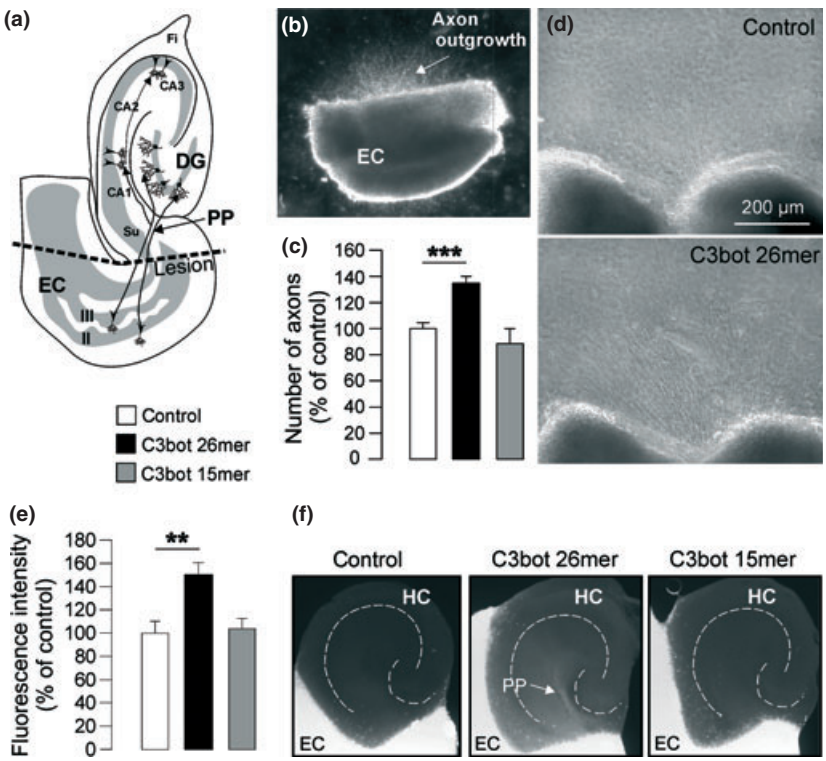

Fig. 3 C3bot 26mer promotes axon outgrowth and re-innervation in organotypical brain slice cultures. Organotypical brain slices from entorhinal cortex (EC) were cultivated for 48 h with no additions or 50 nM of C3bot 26mer and C3bot 15mer. (a) Schematic drawing of the EC-hippocampus formation with the localization of the cutting lesion. CA: Cornu ammonis; DG: dentate gyrus; Fi: fimbra hippocampi; PP: perforant path; Su: subiculum. (b) Sample picture of an entorhinal cortex explant under dark field illumination. Re-growing perforant path fibers are clearly visible. (c) Analysis of axonal density as measured by the number of outgrowing axons (see Materials and methods section). Values under control conditions were set as 100%. Application of C3bot 26mer, but not C3bot 15mer, resulted in highly significant beneficial effects on axon counts. $N = 3$ or more experiments. Data are shown form $n = 61$ (control), $n = 55$ (C3bot 26mer), and $n = 34$ brain slices (C3bot 15mer) Statistical significance was verified using Student's *t*-test. $^{***}p < 0.001$. (d) Under phase contrast optics outgrowing axons (arrowheads) comprising the perforant path in the intact animal were clearly observable. The micrographs demonstrate an enhanced outgrowth after application of C3bot 26mer. (e) C3bot 26mer, but not C3bot 15mer sigificantly enhanced the moderate re-growth observed under control conditions by 50%. (f) Re-innervation of the hippocampus by perforant path fibers: β-actin-eGFP expressing entorhinal cortex (EC) from a transgenic mouse was co-cultured with a littermate wild-type hippocampus (HC). Ingrowth of green fluorescent axons of the perforant path (PP) to the HC was followed after application of C3bot 26mer or C3bot 15mer (both at 50 nM) for 48 h. $n = 12$ (control), $n = 10$ (26mer), $n = 13$ (15mer). Statistical significance was verified using Student's *t*-test. $^{**}p < 0.005$.

regain of motor function in the BMS open field test (Basso *et al.* 1995) and Rotarod experiments as a forced movement test system. Animals were operated and gel-foam patches soaked with 5 μL of 40 μM C3bot 26mer (~790 ng/animal) or PBS were applied directly at the injury site on top of the perforated dura. The gelfoam patch remained in the animals for the entire time of investigation. According to the BMS behavioural tests, animals treated with the peptide showed an improved recovery from both types of injury than mice that received PBS only (Fig. 4a and b). After both contusion injury and spinal hemisection, mice gained relatively constant score points two weeks after surgery. Mice treated with C3bot 26mer reached values 1.5 score points higher than the control group. As previously shown (Boato *et al.* 2010) this model of dorsal hemisection in general represented a more severe form of lesion. A beneficial effect of the C3bot peptide on locomotor recovery was also detectable in the Rotarod experiments, and in case of hemisection it reached significance (Fig. 4c and d). Following hemisection, motor performance of either group was more affected than after contusion injury, confirming the BMS data.

For the 29mer, enhanced recovery of motor function following SCI was reflected by an improved serotonergic input to lumbar motoneurons, a part of them being engaged in hind limb muscle control (Boato *et al.* 2010). In this context, we asked whether incubation with C3bot 26mer (and C3bot 29mer) also had an effect on inhibitory GABA- and glycinergic input to these neurons after spinal hemisection. In this injury model fiber tracts are transected and allow for the study of neuronal plasticity and regeneration. Following completion of the behavioural experiments shown before, spinal cord sections were stained for the vesicular GABA / glycine transporter VGAT and 5-HT. First, we counted VGAT-positive spots contacting the somata of lumbar α-motoneurons at levels L1-L2 in the ventral horn (Fig. 5a and b). However, no detectable alterations in the average number of inhibitory inputs were detected after treatment with C3bot 26mer. This holds true also for C3bot 29mer (data not shown). On the other hand, quantification of serotonergic boutons contacting these motoneurons revealed a 2-fold increase after treatment with this peptide (Fig. 5c).

Next, we addressed the question whether treatment with C3bot peptides impacts on RhoA activation in the spinal

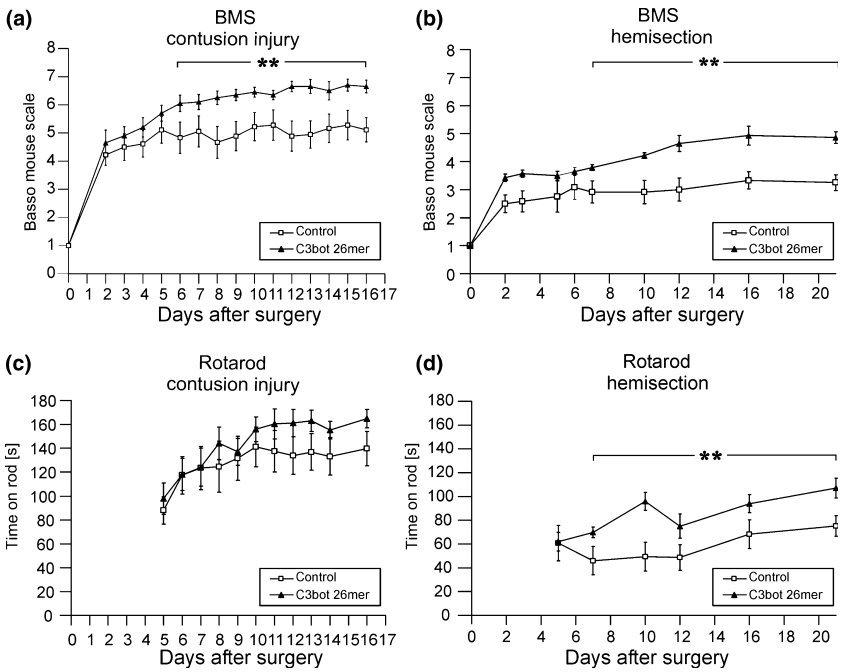

Fig. 4 Local application of C3bot 26mer improves locomotor restoration following spinal cord injury by compression or hemisection. Mice were subjected to two different experimental spinal cord injury (SCI) models. At thoracic level T8, either a compression injury or a dorsal hemisection were conducted. Mice were allowed to recover for approximately three weeks. The regain of motor function was evaluated by open field and forced movement tests. (a, b) C3bot 26mer application (40 μM/5 μL) significantly increased the performance according to the Basso Mouse Scale using either lesion paradigm. Note that hemisection resulted in a more severe motor impairment. Statistical significance was verified using two-way ANOVA. compression: ***F6–16 (1, 10) = 2,589; $p < 0.001$; $n = 9$ (PBS), $n = 10$ (26mer); hemisection: ***F7–21 (1, 5) = 3,517; $p < 0.0001$; $n = 6$ (PBS), 7 (26mer). (c, d) Motor restoration according to Rotarod experiments starting five days after injury. C3bot 26mer application increased the latency time until mice jumped off the Rotarod especially following hemisection. Two-way ANOVA: **F7–21(1, 5) = 4,21; $p < 0.001$; $n = 6$ (PBS), $n = 7$ (26mer).

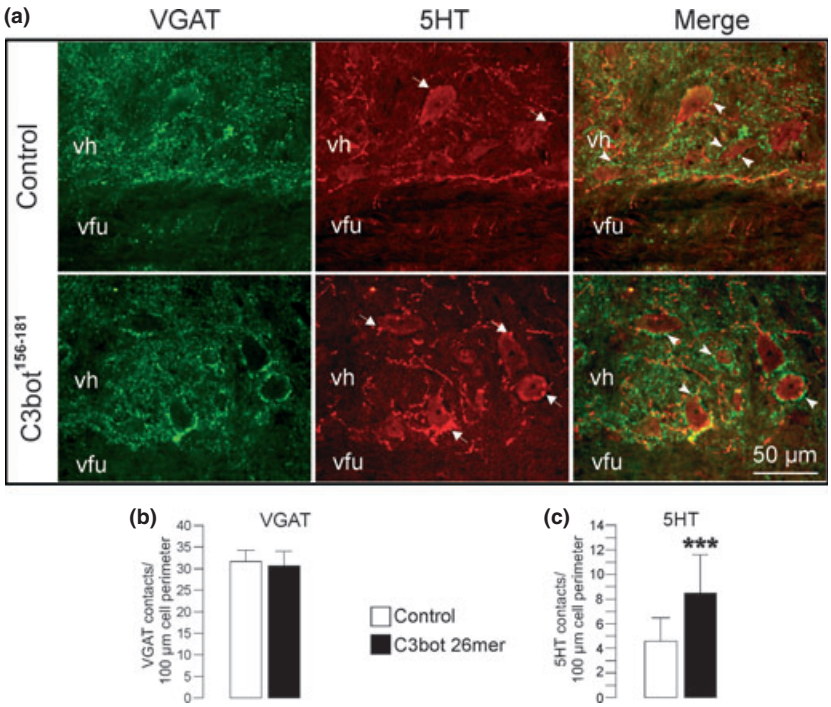

Fig. 5 C3bot 26mer enhances the number of 5HT-positive boutons contacting lumbar α-motoneurons. (a) Photomicrographs showing double staining for VGAT and serotonin (5-hydroxytryptamine, 5-HT) at lumbar segments L1–L2 from mice injured by spinal cord hemisection (treated with PBS for control or C3bot 26mer) 3 weeks after injury. Arrowheads depict VGAT contacts on α-motoneurons, arrows show 5-HT contacts. vh: ventral horn; vfu: ventral funiculus. (b) Quantification of VGAT contacts to lumbar α-motoneurons normalized to the cell body perimeter. C3bot 26mer did not alter the number of inhibitory contacts. $N = 4$ (control) and 3 animals (C3bot 26mer). Data shown are from 16 sections (control) and 13 sections (C3bot 26mer). (c) The number of 5HT-positive boutons was analyzed for C3bot 26mer. In contrast to VGAT contacts, the counts of 5-HT contacts were enhanced by C3bot 26mer. $N = 3$ animals (control and C3bot 26mer). 13 sections (control) and 12 sections (C3bot 26mer) were analyzed. Statistical significance was verified using Student's *t*-test. ***$p < 0.001$.

cord after lesion. This issue was tested for the hemisection model. By performing pull-down assays we analysed active (GTP-bound) RhoA levels from lysates of spinal cord fragments that included the lesion area (Fig. 6a) or the laminectomy site in sham-operated animals. Two time points were chosen, one at 24 h and the other at 7 days after surgery. In addition to C3bot 26mer, C3bot 29mer was also tested *in vivo* because of its known effect on RhoA activation *in vitro*.

As expected, active RhoA (RhoA-GTP) showed a tendency to be up-regulated 24 h after surgery compared with sham-operated mice that exhibited only weak RhoA-GTP signals (Fig. 6b and c). However, the two peptides did not clearly affect RhoA activation. However, RhoA activation was still prominent 7 days after surgery in PBS animals but was clearly reduced in mice that received treatment with C3bot 26mer or 29mer (Fig. 6b and c).

In conclusion, we were able to show in this study that a fragment of C3bot covering 26 amino acid residues is able to stimulate neuronal outgrowth and connectivity in different *in vitro* and *in vivo* systems. A further truncation of the fragment to 15 amino acid residues largely constricts the neuronal growth promoting effects. Other peptides were completely inactive in the experimental settings applied.

Discussion

The primary goal of the present study was to investigate the minimum length of *Clostridium botulinum* C3 transferase to sufficiently exhibit beneficial effects on neuronal process growth, connectivity and regeneration following CNS lesion. Additionally, interactions with putative downstream partners such as the small GTPase RhoA, generally considered as a negative regulator of neuronal regeneration, were examined. The data reveal that a 26-amino acid fragment from C3bot encompassing the residues 156–181 is sufficient to produce promoting effects in a wide range of experimental settings dealing with neuronal growth and interaction. Behavioural experiments indicate that treatment of SCI-injured mice with this fragment results in improved locomotor restoration probably involving C3bot peptide-mediated reduced RhoA activation in the spinal cord. Further shortening of the peptide resulted in partial or even complete loss of activity in the applications tested.

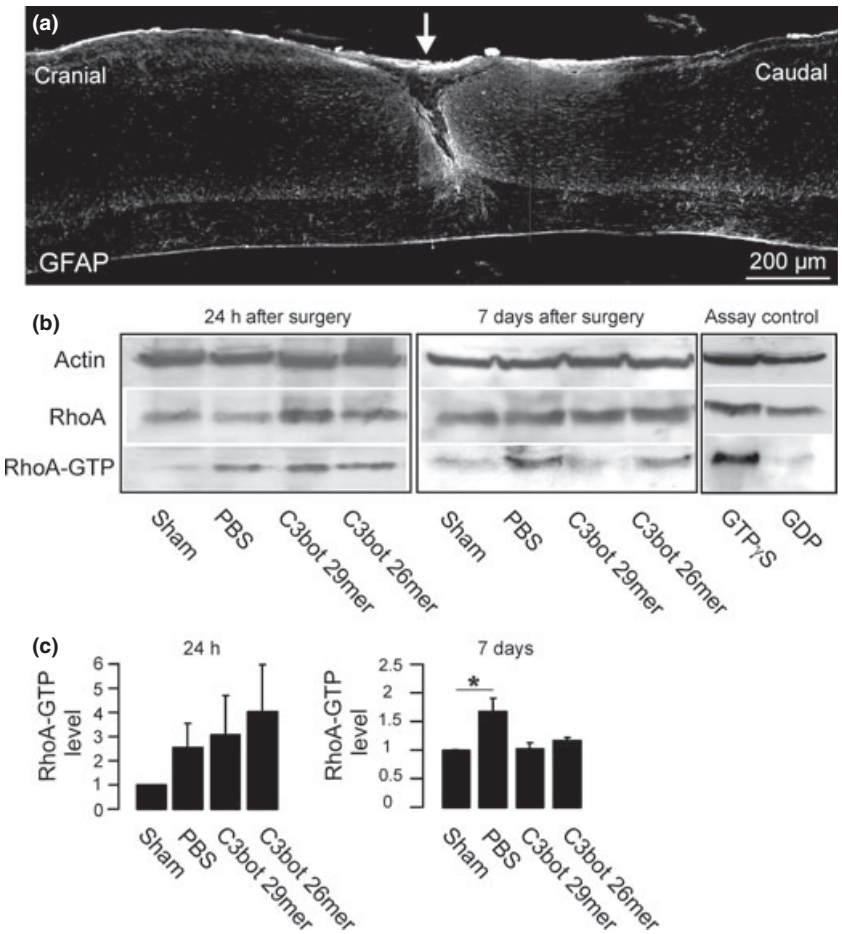

Fig. 6 Prevention of sustained RhoA activation by C3bot peptides C3bot 26mer and 29mer. RhoA pull-down experiments were performed from spinal cord lysates to investigate the influence of C3bot peptides on active RhoA levels following spinal cord injury by hemisection. (a) Photomicrograph illustrating the lesion generated by hemisection. A longitudinal spinal cord section was stained for glial acidic fibrillary protein (GFAP), an astroglial marker used to visualize the lesion. Pieces of the spinal cord that included the lesion area (arrow) were used for pull-down experiments. (b) Spinal cord fragments were obtained from mice injured by spinal cord injury 24 h or 7 days following surgery. Tissue lysates were subjected to rhotekin pull-down assays to detect active RhoA levels (RhoA-GTP). Active RhoA levels were increased 24 h after surgery in PBS, 29mer-(C3bot$^{154-182}$), and C3bot 26mer-treated mice compared with sham-operated animals. Sustained RhoA activation was still detected one week after injury in PBS animals, which was reduced in mice treated with the C3bot peptides. Proper assay function was controlled by addition of the non-hydrolyzable G protein activator GTPγS as positive control and GDP as negative control to lysates from a sham-operated mouse. (c) Quantification of RhoA-GTP levels by LabImage software (Kapelan Bio-Imaging GmbH, Leipzig, Germany). RhoA signals were calculated and normalized to actin signals used as loading controls. $N = 3$ animals for each condition. Statistical significance was verified using Student's *t*-test with $^*p < 0.05$.

Morphological measurements

First, we addressed the question whether the exact amino acid sequence covering the so-called ARTT-loop (Han *et al.* 2001) included in all the peptides used is essential even for its non-enzymatic action. Application of C3bot 29mer with glutamate 174 exchanged still exhibited promoting effects on process elongation comparable to the initially designed 29mer, effects by the modified 29mer on axonal and dendritic branching, however, were not significant (for comparison, see Höltje *et al.* 2009). Noteworthy, elongation and branching crucial for network assembly are distinct mechanisms that are differentially regulated (Kalil *et al.* 2000; Hall and Lalli 2010). Branching mechanisms often include Rac activity (Albertinazzi *et al.* 1998) and Cdc42-governed filopodia extension (Kakimoto *et al.* 2006) that are obviously not affected by this peptide. For dendrite branching, that was promoted by C3bot 26mer, it was shown that activated RhoA acts to inhibit expression of a protein named cypin and, by doing so, decreases dendrite complexity (Chen and Firestein 2007).The observation that C3bot 12mer (identical to the ARTT loop) representing the shortest peptide used exhibited no activity on cultured neurons

further underlines the fact that the exact ARTT loop alone is not sufficient for enzyme-independent neurotrophic action. Also, regions closer to the C-terminal end of C3bot do not seem to contribute to the beneficial effects because the C-terminal 31mer was without effects. An open question remains, why the 15mer, but not the 20mer, exhibited axonotrophic activity. This was surprising, since the 20mer includes the 15mer sequence. Most likely the three-dimensional structure of the peptide or the property to dimerize/oligomerize is the basis for the axonotrophic activity.

We were able to show that C3bot 26mer (and C3bot 29mer) can inhibit RhoA activation. The fact, that C3bot 26mer promotes axon outgrowth and re-innervation in organotypical culture systems further strengthens the data already obtained for the 29mer (Höltje *et al.* 2009) and confirms the effects observed in dissociation culture for more complex culture systems. Interestingly, the 15-amino acid fragment was without effect in brain slice culture despite its effectiveness on axon growth in primary dissociation culture. Given the working hypothesis that C3bot peptides bind to a neuronal receptor structure to achieve their effects (reviewed in Just *et al.* 2011) one must assume that the 15mer falls below a critical length for acting as a ligand, at least for receptors expressed on the surface of neurons cultivated in their organotypical context, obtained from postnatal animals (dissociation cultures represent neurons prepared at embryonic stage).

Synaptic connectivity

Analysis of synaptic connectivity in primary culture revealed promoting effects of C3bot 26mer, but not C3bot 15mer (or other peptides ineffective also in morphometrical measurements) on the number of synaptic inputs. The observed higher number of synaptic contacts corresponds with the increased dendritic length and branching detected after application of C3bot 26mer, a phenomenon that was not seen in cultures treated with C3bot 15mer. The effects on synaptophysin and Map2 elicited by the 26mer were also evident when analysed by Western blot analysis. Moreover, treatment with C3bot 26mer prevented CSPG-mediated down-regulation of synaptic inputs. Inhibitory effects of extracellular matrix components such as CSPG achieve their inhibitory effects on neuronal growth largely by signalling pathways which converges on RhoA activation (Schweigreiter *et al.* 2004). In accordance to our observations for axonal and dendritic growth of cultivated hippocampal neurons in the current study and in our earlier observation (Boato *et al.* 2010), it was shown that CSPG treatment can result in a strong reduction of neuronal growth by up to 50% (Shen *et al.* 2009). So, it appears very likely that the observed reduced synaptic input in cultures grown on CSPG without peptide reflects the reduced possibility to establish interneuronal connections in the absence of an extensive network of neuronal processes. However, impairment of RhoA signalling by C3bot 26mer seems to be a likely mechanism by which its beneficial effects on (functional) neuronal outgrowth are achieved.

In addition to the *in vitro* experiments, effects of C3bot 26mer on neuronal connectivity were also investigated for the input to lumbar α-motoneurons after spinal cord injury in mice. In a previous study we were able to show that application of $C3bot^{154-182}$ (C3bot 29mer) enhances the number of regenerating corticospinal fibers following thoracic SCI (Boato *et al.* 2010). Complementing the improved regenerational growth of glutamatergic corticospinal fibers (Rekling *et al.* 2000), we detected a higher number of serotonergic inputs to lumbar motoneurons in animals treated with C3bot 29mer. Serotonergic brainstem fibers set spinal motoneurons in an excitable state rendering them ready to cause muscle contraction mainly by activation of $5\text{-}HT_{2C}$ receptors, regulating persisting Ca^{2+} and Na^{+} currents (Li *et al.* 2007; Murray *et al.* 2010). In the present study, we could show a positive effect for C3bot 26mer on serotonergic input to lumbar α-motoneurons, but we were unable to detect changes in inhibitory GABAergic/glycinergic input to these neurons in mice treated with C3bot 26mer. One possible explanation for this differential outcome might be that the peptides were applied locally at the site of spinal cord injury (T8) 6–7 segments above the localization of the lumbar motoneurons (L1–L2). By using this form of application descending fibers that pass or regenerate through the thoracic lesion area might benefit from the peptide effect, rather than inhibitory fibers originating from local inhibitory interneurons localized to lumbar segments.

Clinical outcome after spinal cord injury

In this study, we used two different models of experimental spinal cord injury, compression injury and hemisection. While the former reflects the most frequent type of injury in humans (Sekhon and Fehlings 2001), the latter might produce a more defined lesion and is better suited to study truly regenerating fibers. The behavioural data clearly show an improved recovery of the treatment group (C3bot 26mer) compared with the control group after either form of lesion. This could reflect an increase in the intrinsic plasticity of the spinal cord axons resulting in regeneration of axotomized axons or collateral sprouting of unlesioned tracts. Alternatively, the effects could be due to enhanced sparing of spinal tissue, particularly in the case of the compression injury. Moreover, it can be assumed that the observed increase in serotonergic input to lumbar motoneurons in mice which underwent hemisection, results from enhanced regenerative growth of raphespinal fibers or increased neuroprotection mediated by the peptide, as observed in the case of C3bot 29mer (Boato *et al.* 2010). A dominant role of serotonin for spinal motoneuron excitability has been demonstrated repeatedly (Harvey *et al.* 2006; Ung *et al.* 2008; Boido *et al.* 2009).

C3bot peptides and RhoA activation

Despite the lack of ADP-ribosylating activity, C3bot peptide-mediated effects on neuronal outgrowth still seem to be based on Rho-dependent signaling mechanisms. Evidence for this comes from pull-down studies that detected a reduced RhoA activation in spinal cord tissue one week after experimental SCI in mice treated with C3bot 26mer and 29mer. Up-regulation of Rho proteins following SCI is considered to be a p75 neurotrophin receptor-dependent process and represents a hallmark in the cellular responses to this type of injury (Yamashita and Tohyama 2003; Conrad *et al.* 2005; McKerracher and Higuchi 2006). Increased levels of activated RhoA seem to account to a great extent for axonal growth-inhibition following CNS lesions. So far, the exact molecular events resulting in RhoA inhibition by C3bot peptides remain elusive. Putative mechanisms include binding to a neuronal receptor to trigger intracellular signaling pathways. Alternatively, a putative receptor would only mediate uptake of C3bot peptides to act in an intracellular way. A direct non-enzymatic interaction of C3bot with intracellular targets was shown for the small GTPase RalA (Wilde *et al.* 2002), but can be excluded for C3bot peptides (I. Just, unpublished observations). Nevertheless, non-enzymatic interaction of C3bot peptides with RhoA is also detectable in cultured hippocampal neurons (Boato *et al.* 2010) leading to the assumption that this indeed represents a general mechanism of action to promote neuronal outgrowth by short C3bot-derived peptides.

Overall, the present study clearly demonstrates the high potential of the 26-amino acid peptide C3bot$^{156-181}$ to stimulate the limited intrinsic repair mechanisms in the CNS after lesion. Further truncation of the peptide sequence results in substantial loss of function. It is conceivable, that the length of the peptides defines the range of activated cellular effectors. Compared with the use of wild-type C3 exoenzyme, the use of neuron-specific enzyme-deficient C3 peptides to stimulate neuronal growth processes seems to be favourable especially in the *in vivo* situation. Observations from our laboratory showed that application of C3bot wild type at equimolar dose to C3bot peptides after SCI resulted in serious unwanted side effects including death in half of the animals tested. Although the detailed reasons for this observation yet remain to be determined, it is tempting to assume that they are linked to ubiquitous effects mediated by C3bot on various cell types not shared by C3bot peptides.

Acknowledgements

The authors are indebted to Birgit Metze, Annemarie Löchner and Julia König for their engaged and skillful technical assistance. Work was supported by grants from the Deutsche Forschungsgemeinschaft (DFG) to MH and GAH (HO 3249/2–1), IJ (JU 231/5–1) and SH (SPP1394). This study was also supported in part by grants from the Berlin-Brandenburg Center for Regenerative Therapies and the Flemish Research Council (FWO) to SH. All authors declare no conflicts of interest.

Supporting information

Additional supporting information may be found in the online version of this article:

Figure S1. Treatment with C3bot 20mer or C3bot 12mer does not alter synaptic connectivity in hippocampal neurons.

As a service to our authors and readers, this journal provides supporting information supplied by the authors. Such materials are peer-reviewed and may be re-organized for online delivery, but are not copy-edited or typeset. Technical support issues arising from supporting information (other than missing files) should be addressed to the authors.

References

Ahnert-Hilger G., Höltje M., Grosse G., Pickert G., Mucke C., Nixdorf-Bergweiler B., Boquet P., Hofmann F. and Just I. (2004) Differential effects of Rho GTPases on axonal and dendritic development in hippocampal neurones. *J. Neurochem.* **90**, 9–18.

Aktories K. and Just I. (2005) Clostridial Rho-inhibiting protein toxins. *Curr. Top. Microbiol. Immunol.* **291**, 113–145.

Albertinazzi C., Gilardelli D., Paris S., Longhi R. and de Curtis I. (1998) Overexpression of a neural-specific rho family GTPase, cRac1B, selectively induces enhanced neuritogenesis and neurite branching in primary neurons. *J. Cell Biol.* **142**, 815–825.

Basso D. M., Beattie M. S. and Bresnahan J. C. (1995) A sensitive and reliable locomotor rating scale for open field testing in rats. *J. Neurotrauma* **12**, 1–21.

Basso D. M., Fisher L. C., Anderson A. J., Jakeman L. B., McTigue D. M. and Popovich P. G. (2006) Basso Mouse Scale for locomotion detects differences in recovery after spinal cord injury in five common mouse strains. *J. Neurotrauma* **23**, 635–659.

Bertrand J., Di Polo A. and McKerracher L. (2007) Enhanced survival and regeneration of antagonists. *Neurobiol. Dis.* **25**, 65–72.

Boato F., Hendrix S., Huelsenbeck S. C. *et al.* (2010) C3 peptide enhances recovery from spinal cord injury by improved regenerative growth of descending fiber tracts. *J. Cell Sci.* **123**, 1652–1662.

Boido M., Rupa R., Garbossa D., Fontanella M., Ducati A. and Vercelli A. (2009) Embryonic and adult stem cells promote raphespinal axon outgrowth and improve functional outcome following spinal hemisection in mice. *Eur. J. Neurosci.* **30**, 833–846.

Chen H. and Firestein B. L. (2007) RhoA regulates dendrite branching in hippocampal neurons by decreasing cypin protein levels. *J. Neurosci.* **27**, 8378–8386.

Conrad S., Schluesener H. J., Trautmann K., Joannin N., Meyermann R. and Schwab J. M. (2005) Prolonged lesional expression of RhoA and RhoB following spinal cord injury. *J. Comp. Neurol.* **487**, 166–175.

Dergham P., Ellezam B., Essagian C., Avedissian H., Lubell W. D. and McKerracher L. (2002) Rho signaling pathway targeted to promote spinal cord repair. *J. Neurosci.* **22**, 6570–6577.

Dubreuil C. I., Winton M. J. and McKerracher L. (2003) Rho activation patterns after spinal cord injury and the role of activated Rho in apoptosis in the central nervous system. *J. Cell Biol.* **162**, 233–243.

Hall A. and Lalli G. (2010) Rho and Ras GTPases in axon growth, guidance, and branching. *Cold Spring Harb. Perspect. Biol.* **2**, a001818.

Han S., Arvai A. S., Clancy S. B. and Tainer J. A. (2001) Crystal structure and novel recognition motif of rho ADP-ribosylating C3

exoenzyme from Clostridium botulinum: structural insights for recognition specificity and catalysis. *J. Mol. Biol.* **305**, 95–107.

Harvey P. J., Li X., Li Y. and Bennett D. J. (2006) 5-HT2 receptor activation facilitates a persistent sodium current and repetitive firing in spinal motoneurons of rats with and without chronic spinal cord injury. *J. Neurophysiol.* **96**, 1158–1170.

Hechler D., Nitsch R. and Hendrix S. (2006) Green-fluorescent-protein-expressing mice as models for the study of axonal growth and regeneration in vitro. *Brain Res. Rev.* **52**, 160–169.

Hechler D., Boato F., Nitsch R. and Hendrix S. (2010) Differential regulation of axon outgrowth and reinnervation by neurotrophin-3 and neurotrophin-4 in the hippocampal formation. *Exp. Brain Res.* **205**, 215–221.

Henneberger C., Jüttner R., Schmidt S. A., Walter J., Meier J. C., Rothe T. and Grantyn R. (2005) GluR- and TrkB-mediated maturation of GABA receptor function during the period of eye opening. *Eur. J. Neurosci.* **2**, 431–440.

Höltje M., Djalali S., Hofmann F. *et al.* (2009) A 29-amino acid fragment of Clostridium botulinum C3 protein enhances neuronal outgrowth, connectivity, and reinnervation. *FASEB J.* **23**, 1115–1126.

Jin Z. and Strittmatter S. M. (1997) Rac1 mediates collapsin-1-induced growth cone collapse. *J. Neurosci.* **17**, 6256–6263.

Just I., Rohrbeck A., Huelsenbeck S. C. and Hoeltje M. (2011) Therapeutic effects of Clostridium botulinum C3 exoenzyme. *Naunyn Schmiedebergs Arch. Pharmacol.* **383**, 247–252.

Kakimoto T., Katoh H. and Negishi M. (2006) Regulation of neuronal morphology by Toca-1, an F-BAR/EFC protein that induces plasma membrane invagination. *J. Biol. Chem.* **281**, 29042–29053.

Kalil K., Szebenyi G. and Dent E. W. (2000) Common mechanisms underlying growth cone guidance and axon branching. *J. Neurobiol.* **44**, 145–158.

Lehmann M., Fournier A., Selles-Navarro I., Dergham P., Sebok A., Leclerc N., Tigyi G. and McKerracher L. (1999) Inactivation of Rho signaling pathway promotes CNS axon regeneration. *J. Neurosci.* **19**, 7537–7547.

Li X., Murray K., Harvey P. J., Ballou E. W. and Bennett D. J. (2007) Serotonin facilitates a persistent calcium current in motoneurons of rats with and without chronic spinal cord injury. *J. Neurophysiol.* **97**, 1236–1246.

McKerracher L. and Higuchi H. (2006) Targeting Rho to stimulate repair after spinal cord injury. *J. Neurotrauma* **23**, 309–317.

Ménétrey J., Flatau G., Boquet P., Ménez A. and Stura E. A. (2008) Structural basis for the NAD-hydrolysis mechanism and the ARTT-loop plasticity of C3 exoenzymes. *Protein Sci.* **17**, 878–886.

Müllner A., Gonzenbach R. R., Weinmann O., Schnell L., Liebscher T. and Schwab M. E. (2008) Lamina-specific restoration of serotonergic projections after Nogo-A antibody treatment of spinal cord injury in rats. *Eur. J. Neurosci.* **27**, 326–333.

Murray K. C., Nakae A., Stephens M. J. *et al.* (2010) Recovery of motoneuron and locomotor function after spinal cord injury depends on constitutive activity in 5-HT2C receptors. *Nat. Med.* **16**, 694–700.

Rekling J. C., Funk G. D., Bayliss D. A., Dong X. W. and Feldman J. L. (2000) Synaptic control of motoneuronal excitability. *Physiol. Rev.* **80**, 767–852.

Schmitt K. R., Kern C., Lange P. E., Berger F., Abdul-Khaliq H. and Hendrix S. (2007) S100B modulates IL-6 release and cytotoxicity from hypothermic brain cells and inhibits hypothermia-induced axonal outgrowth. *Neurosci. Res.* **59**, 68–73.

Schmitt K. R., Boato F., Diestel A., Hechler D., Kruglov A., Berger F. and Hendrix S. (2010) Hypothermia-induced neurite outgrowth is mediated by tumor necrosis factor-alpha. *Brain Pathol.* **20**, 771–779.

Schweigreiter R., Walmsley A. R., Niederöst B., Zimmermann D. R., Oertle T., Casademunt E., Frentzel S., Dechant G., Mir A. and Bandtlow C. E. (2004) Versican V2 and the central inhibitory domain of Nogo-A inhibit neurite growth via p75NTR/NgR-independent pathways that converge at RhoA. *Mol. Cell. Neurosci.* **27**, 163–174.

Sekhon L. H. and Fehlings M. G. (2001) Epidemiology, demographics, and pathophysiology of acute spinal cord injury. *Spine* **26**(24 Suppl.) 2–12.

Shen Y., Tenney A. P., Busch S. A., Horn K. P., Cuascut F. X., Liu K., He Z., Silver J. and Flanagan J. G. (2009) PTPsigma is a receptor for chondroitin sulfate proteoglycan, an inhibitor of neural regeneration. *Science* **326**(5952), 592–596.

Sheng H., Wang H., Homi H. M., Spasojevic I., Batinic-Haberle I., Pearlstein R. D. and Warner D. S. (2004) A no-laminectomy spinal cord compression injury model in mice. *J. Neurotrauma* **21**, 595–603.

Sieber-Blum M., Schnell L., Grim M., Hu Y. F., Schneider R. and Schwab M. E. (2006) Characterization of epidermal neural crest stem cell (EPI-NCSC) grafts in the lesioned spinal cord. *Mol. Cell. Neurosci.* **32**, 67–81.

Simonen M., Pedersen V., Weinmann O., Schnell L., Buss A., Ledermann B., Christ F., Sansig G., van der. Putten. H. and Schwab M. E. (2003) Systemic deletion of the myelin-associated outgrowth inhibitor Nogo-A improves regenerative and plastic responses after spinal cord injury. *Neuron* **38**, 201–211.

Ung R. V., Landry E. S., Rouleau P., Lapointe N. P., Rouillard C. and Guertin P. A. (2008) Role of spinal 5-HT2 receptor subtypes in quipazine-induced hindlimb movements after a low-thoracic spinal cord transection. *Eur. J. Neurosci.* **28**, 2231–2242.

Vogelsgesang M., Pautsch A. and Aktories K. (2007) C3 exoenzymes, novel insights into structure and action of Rho-ADP-ribosylating toxins. *Naunyn Schmiedebergs Arch. Pharmacol.* **374**, 347–360.

Wilde C., Barth H., Sehr P., Han L., Schmidt M., Just I. and Aktories K. (2002) Interaction of the Rho-ADP-ribosylating C3 exoenzyme with RalA. *J. Biol. Chem.* **277**, 14771–14776.

Yamashita T. and Tohyama M. (2003) The p75 receptor acts as a displacement factor that releases Rho from Rho-GDI. *Nat. Neurosci.* **6**, 461–467.